Biomaterials 32 (2011) 2043–2051

Contents lists available at ScienceDirect

Biomaterials

journal homepage: www.elsevier.com/locate/biomaterials

The regulation of traction force in relation to cell shape and focal adhesions

Andrew D. Rape, Wei-hui Guo, Yu-li Wang*

Department of Biomedical Engineering, Carnegie Mellon University, PTC 4105-07, 700 Technology Drive, Pittsburgh, PA 15219, USA

ARTICLE INFO

Article history:
Received 2 November 2010
Accepted 18 November 2010
Available online 15 December 2010

Keywords:
Microcontact printing
Polyacrylamide
Traction force
Cell shape

ABSTRACT

Mechanical forces provide critical inputs for proper cellular functions. The interplay between the generation of, and response to, mechanical forces regulate such cellular processes as differentiation, proliferation, and migration. We postulate that adherent cells respond to a number of physical and topographical factors, including cell size and shape, by detecting the magnitude and/or distribution of traction forces under different conditions. To address this possibility we introduce a new simple method for precise micropatterning of hydrogels, and then apply the technique to systematically investigate the relationship between cell geometry, focal adhesions, and traction forces in cells with a series of spread areas and aspect ratios. Contrary to previous findings, we find that traction force is not determined primarily by the cell spreading area but by the distance from cell center to the perimeter. This distance in turn controls traction forces by regulating the size of focal adhesions, such that constraining the size of focal adhesions by micropatterning can override the effect of geometry. We propose that the responses of traction forces to center-periphery distance, possibly through a positive feedback mechanism that regulates focal adhesions, provide the cell with the information on its own shape and size. A similar positive feedback control may allow cells to respond to a variety of physical or topographical signals via a unified mechanism.

1. Introduction

The shape of adherent cells is known to have profound effects on a number of important properties including cytoskeletal structure, growth, and differentiation [1–4]. When allowed to adhere and spread without constraints, most adhesive cells reach an extended polygonal shape and form large cables of actin filaments, accompanied by active DNA synthesis and growth [1]. Using patterned substrates to control cell shape, it was discovered that the rate of fibroblast growth increases with the spreading area [1,5]. More importantly, spreading area appears to control the differentiation of stem cells. Human mesenchymal stem cells allowed to spread over a large area differentiate into osteocytes, whereas those confined within small areas differentiate into adipocytes [6]. In addition to spreading area, aspect ratio has also been found to affect the differentiation of mesenchymal stem cells [7].

Despite the significance, how shape information is transduced into intracellular chemical signals remains largely unclear. An important clue is that shape-dictated differentiation requires RhoA-dependent contractility of the actin cytoskeleton, which is known to generate "traction forces" – mechanical forces exerted by adherent cells on the underlying substrate [8–10]. Therefore, an attractive possibility is that traction forces are involved in reading out cell shape. Consistent with this hypothesis, responses of adherent cells to cell geometry share similarities to those elicited by applied mechanical forces, including the reinforcement of the actin cytoskeleton and focal adhesions [11,12] and the activation of similar signaling pathways [13,44]. In addition, traction forces were found to increase with the cell spreading area [15–19]. Since traction forces are actively generated near the leading edge [20–23], their distribution and magnitude may respond to cell shape and serve as the readout as cells actively change their geometry.

The goal of this study is to identify the aspect of cell shape that determines the responses and the structural basis of the readout mechanism. Previous studies have been limited by technical challenges, specifically difficulties in micro-patterning soft gels for traction force measurements under controlled geometry [17]. To address the challenge we have developed a novel method that allows easy and reproducible generation of adhesive micropatterns on hydrogels at a high resolution. We then applied this approach to systematically investigate the role of cellular geometry in traction force regulation by varying the area, aspect ratio, and adhesion pattern of cells in various rectangular shapes. The knowledge of how cells sense and respond to their own shape should provide

* Corresponding author. Tel.: +1 412 268 4442.
E-mail address: yuliwang@andrew.cmu.edu (Y.-l. Wang).

0142-9612/$ – see front matter © 2010 Elsevier Ltd. All rights reserved.
doi:10.1016/j.biomaterials.2010.11.044

the field of tissue engineering with a diverse toolbox for controlling cellular fate when combined with other chemical and mechanical manipulations.

2. Methods

2.1. Preparation of patterned polyacrylamide hydrogels

A novel patterning method was developed for patterning polyacrylamide hydrogels. Initially, 50 bloom gelatin at a concentration of 0.1% was activated by incubation with 3.6 mg/ml sodium m-periodate (Sigma, St Louis, MO) at room temperature for 30 min, as previously described [24]. Polydimethylsiloxane (PDMS) stamps were fabricated by standard soft lithography procedures. Briefly, a positive photoresist, SPR-220.3 (Microchem, Newton, MA), was spun on a glass coverslip. It was then exposed to UV light through a patterned photomask and developed for use as molding. PDMS pre-polymers (Dow Corning, Midland, MI) were then mixed with catalyst and poured over the coverslip and cured at 60 °C for 1 h. The PDMS stamp was then cut away from the molding and incubated with activated gelatin solution for 30 min. Because of the hydrophobic nature of the PDMS stamp, a thin layer of molecular gelatin adsorbed to the stamp. Excess solution was blown away under a nitrogen stream and the stamp was brought into manual contact with a small square glass coverslip for 5 min, causing the transfer of molecular gelatin to the stamp.

Polyacrylamide was prepared as described previously [25], with a final concentration of 5% acrylamide (BioRad, Hercules, CA), 0.1% bisacrylamide (BioRad), and a 1:1000 dilution of 0.2 μm fluorescent latex beads (Molecular Probes, Carlsbad, CA). 30 μL of this solution, along with initiators ammonium persulfate and N,N,N′,N′ tetramethylethylenediamine (both from BioRad), were pipetted onto a large Bind-Silane (GE Healthcare, Waukesha, WI) activated coverslip. The stamp was removed from the small patterned coverslip and placed patterned side down onto the acrylamide solution. After polymerization was complete, the top coverslip was gently removed. The final gel had an estimated Young's modulus of 5.8 kPa [26].

2.2. Cell culture

Patterned polyacrylamide hydrogels were mounted into chamber dishes and incubated in cell culture media for 30 min at 37 °C. NIH 3T3 cells were cultured in Dulbecco's modified Eagle's medium (Sigma), supplemented with 10% donor calf serum (JHR Biosciences, Lenexa, KS), 2 mM L-glutamine, 50 μg/ml streptomycin, and 50 U/ml penicillin (Gibco-BRL, Gaithersburg, MD). Cells were plated on the hydrogels and allowed to spread overnight.

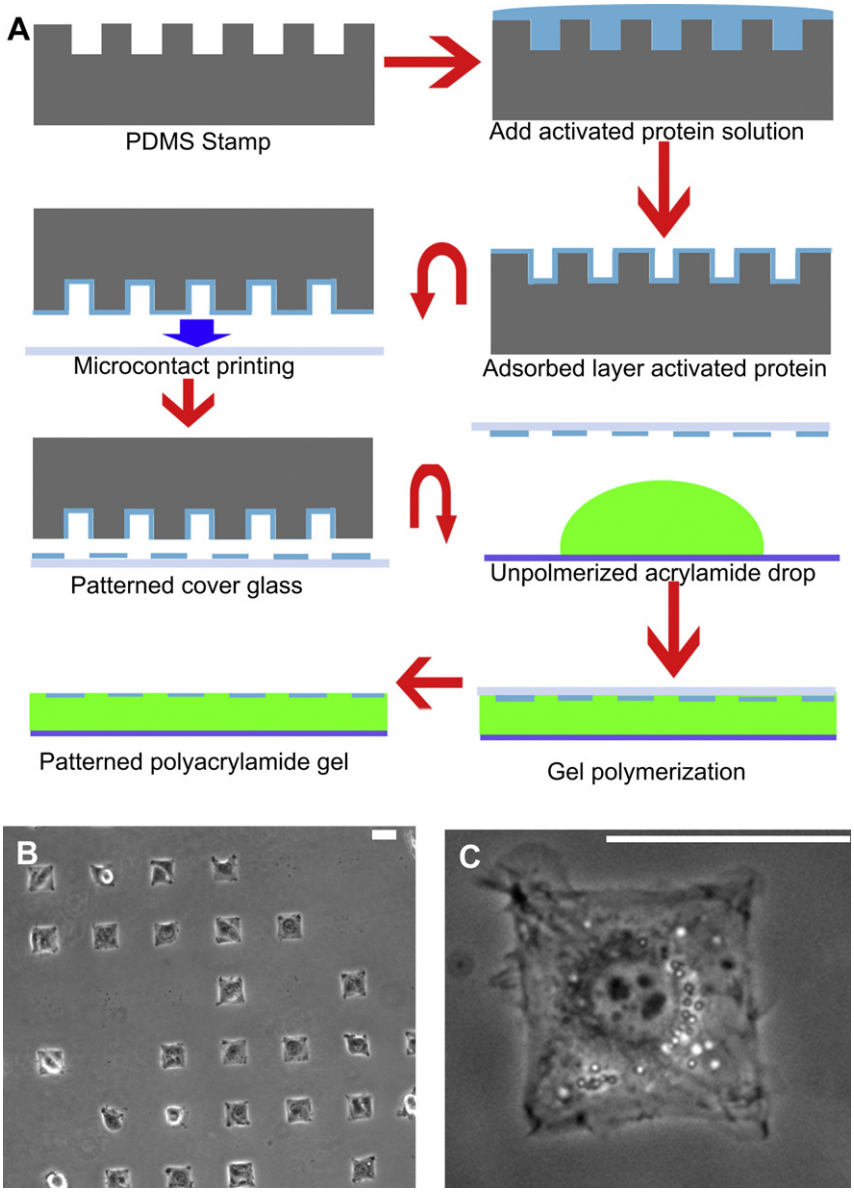

Fig. 1. Schematic diagram of novel polyacrylamide patterning technique. A PDMS stamp is cast on photoresist molding fabricated with standard photolithography. It is inked with activated protein and dried with an inert gas stream. The stamp is then manually brought into contact with a small glass coverslip. Acrylamide solution is prepared and activated as described previously. A small volume is immediately placed onto a Bind-Silane treated coverslip. The stamped coverglass is inverted on top of the polymerizing acrylamide solution to transfer the patterned protein and removed after polymerization is complete.

2.3. Traction force microscopy, immunofluorescence, and image analysis

For traction force microscopy, phase contrast images of single, mono-nucleated cells adhered to an island were collected using an Axiovert S100TV (Carl Zeiss, Thornwood, NY) microscope equipped with a 40× plan neofluar air objective. Only cells that were nearly fully spread to the desired micropatterned domain were chosen for analysis. A fluorescent image of the beads near the ventral surface of the cell was acquired. A second fluorescent image of the beads in relaxed positions was acquired was acquired after removing the cell with a microneedle. Substrate displacement fields and the corresponding traction stress maps were computed as previously described using custom software and the LIBTRC package [[21]; courtesy of Dr. Micah Dembo, Boston University]. In the calculation of traction stresses a boundary condition was imposed that confines traction forces to within the lateral border of the cell. This is a reasonable assumption as there is no physical basis for forces being exerted outside of the cell boundary. Substrate strains outside of cell domain are assumed to be a result of forces exerted inside the cell domain being transferred to the outside region via elastic coupling. Strong traction stress at the corner was quantified as traction stress that was concentrated at the four corners of the cell which comprised a total of 5% of the area of the cell.

Focal adhesion images were obtained by immunofluorescence staining for paxillin after cells were fixed with 4% paraformaldehyde (Electron Microscopy Sciences, Hatfield, PA). Images were collected using an Axiovert 200M (Carl Zeiss) with a QLC100 (Solamere, Salt Lake City, UT) spinning disk confocal attachment and a 40× fluar oil immersion objective and processed with a gradient based segmentation algorithm in MATLAB (The MathWorks, Natick, MA) to identify focal adhesions. Briefly, a Sobel operator was applied to images and thresholded with an empirically determined value. The resulting lines were then dilated to ensure closed shapes, which were then labeled as focal adhesions.

2.4. Statistical analysis

Significance tests for regression slopes were conducted by linear regression analysis. The null hypothesis states that the slope of the relationship between the two groups is 0, indicating that there is not a linear relationship between the two.

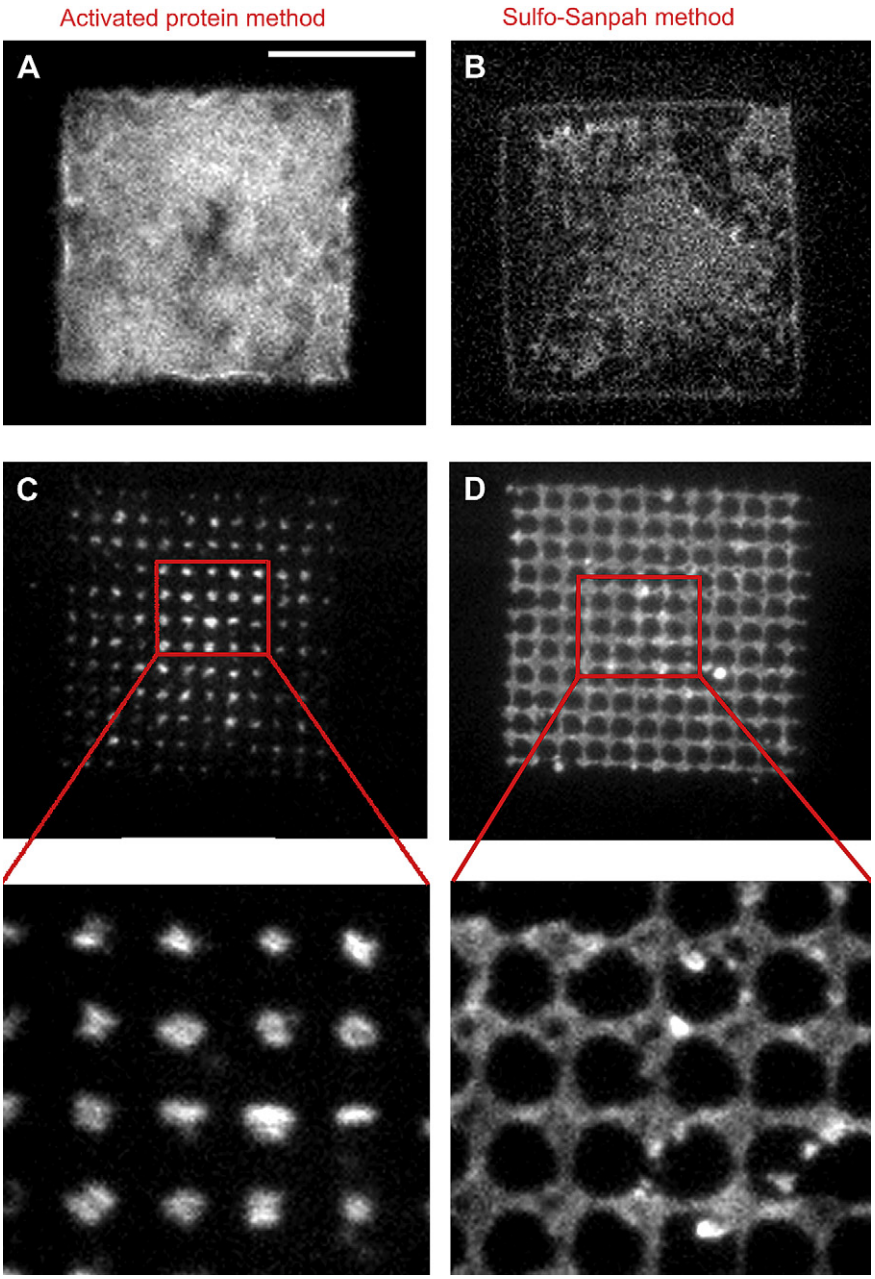

Fig. 2. Comparison of protein pattern generated with the present method to that generated by direct microcontact printing on gel surfaces. Fluorescently tagged fibronectin was patterned as 50 × 50 μm squares using either the present approach (A), or direct microcontact printing on sulfo-SANPAH activated gel surface (B). The present method was able to transfer more protein and cover the adhesive area more completely. It also generated more reproducible patterns and at a higher resolution, as indicated by printing a matrix of 2 μm diameter dots (C, D). Scale bar, 25 μm.

The test statistic, *T*, is the slope estimate divided by its standard deviation. α was set at 0.05. The coefficient of determination for the linear fit was determined using Microsoft Excel.

3. Results

3.1. Developing a new patterning technique for polyacrylamide hydrogels

To address the question of how cell geometry regulates the generation of traction stress, it is essential to constrain cells geometrically on adhesive islands of defined shape cast on elastic hydrogels. Among cell culture suitable materials, protein-conjugated polyacrylamide hydrogels have emerged as an ideal, tunable substrate for many purposes. However, it has been technically challenging to create high-quality adhesive patterns on these non-adhesive gels for controlling cell migration or shape, due to difficulties in microcontact printing on a deformable surface. We have therefore developed a new technique by transferring chemically activated adhesive proteins, patterned at a high resolution on a glass coverslip via microcontact printing (Fig. 1), to the surface of polyacrylamide by inverting the glass on top of a polymerizing acrylamide solution.

Patterning with gelatin in a soluble state resulted in a molecular layer covalently attached to the polyacrylamide surface. The resulting pattern was compared against patterns created by direct microcontact printing onto sulfo-SANPAH activated polyacrylamide gels (Fig. 2). A matrix of small (2 μm diameter) dots over a 50 × 50 μm area was used as the test pattern. The new method was able to reproduce the dot pattern easily and faithfully (Fig. 2C), while direct microcontact printing either transferred only a small fraction of dots when pressed with the same pressure (Fig. 2D), or created smeared dots under increased pressure. Furthermore, the present method was able to maintain the integrity of 92% of 50 × 50 μm squares (Fig. 2A and Table 1), while direct microcontact printing generated a large fraction of incomplete squares (56%; Fig. 2B and Table 1). Quantitative comparison of the amount of protein conjugated on the surface (based on fluorescence intensity of the pattern relative to background intensity) also indicated that the present method is able to deliver proteins to the gel surface approximately five times more efficiently.

Traction forces generated by cells cultured on the patterned surface were detected based on the displacement of fluorescent particles embedded in the gel, as described previously [21]. Only cells that covered at least 95% of the shaped adhesive area were chosen for analysis. Note that while mechanical strains propagated outside the cell due to the coupling across the elastic material (Fig. 2), traction forces must be exerted entirely within the cell border. This was used as part of the boundary conditions for the computation of traction stress [21].

Table 1
Comparison of the performance of the present patterning method with direct microcontact printing onto sulfo-SANPAH activated gels. The present method was able to transfer a significantly larger amount of proteins ($p < 0.00005$, by Student's *T*-Test) and to create a larger percentage of perfect squares (3 trials of 100 squares for each patterning method). Furthermore, the present method took a considerably smaller amount of time. Standard deviations are presented as ±.

	Current method	Direct microcontact printing
Ability to achieve 2 μm resolution	Yes	No
Percentage of perfectly transferred 50 × 50 μm squares	92 ± 2	44 ± 3.6
Relative amount of protein conjugated	0.633 ± 0.178	0.124 ± 0.045
Total estimated time of procedure	~1 h.	~4 h.

3.2. Dissecting the primary parameter for geometry sensing

A set of patterns was designed that systematically and independently varied the area and shape in order to determine the governing parameter of traction forces. We first investigated

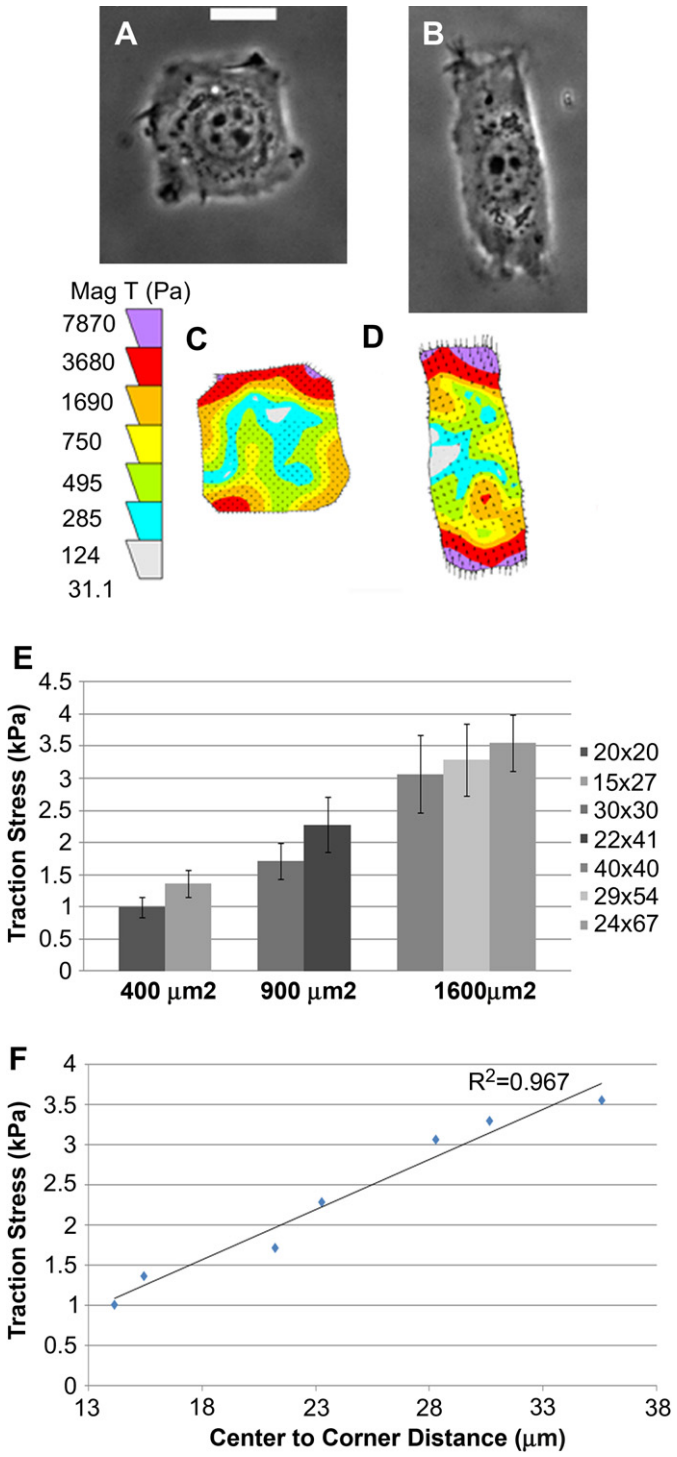

Fig. 3. Dependence of traction stress on cell shape and spreading area. Phase contrast and corresponding traction stress maps of cells patterned on a 40 × 40 μm square (A, C) or 24 × 7 μm rectangle (B, D). The bar graph shows average corner traction stress for cells spreading over various rectangular areas and aspect ratios (E; $n \sim 17$). Each group of bars indicates cells of the same area. Error bars represent SEM. Plotting average corner traction stress against the center-to-corner distance shows a linear relationship regardless of the spreading area (F). The trend is highly significant ($p < 0.0001$) compared to random data.

traction stresses of cells confined to squares of different areas. Cells on squares concentrated strong traction forces at the corners as reported previously [17,19,27–29], therefore average stress in 5% of the area at corners was quantified as the average corner traction stress.

Square cells of increasing areas showed a corresponding increase in the average corner traction stress (Supp. Fig. 1), consistent with previous observations [17,19,27–29]. However this relationship may reflect either a direct dependence of traction stress on cell spreading area itself or a dependence on other co-varying geometric parameters. By plating cells on a set of rectangular patterns of a constant area but different aspect ratios (Fig. 3), we found that average corner traction stress increases with the aspect ratio despite the constant area. In addition, by analyzing the response to a range of cell areas and aspect ratios, we found that average corner traction stress varies linearly with the distance between the cell center and the corner regardless of the cell area ($R^2 = 0.967$). These observations suggest that the primary factor controlling traction forces is not cell spreading area. While it is difficult to rule out other co-varying factors, the key parameter appears to be the distance from the cell center, i.e., the farther a given area extends away from the cell center, the more force it generates.

3.3. Determining the structural basis for geometry sensing

To regulate traction forces as observed above, the distance from the cell center must be translated into structural features or chemical signals. We hypothesized that the total area of focal adhesions serves this function. By analyzing immunofluorescence images of paxillin in cells of different spread areas and shapes, we found that focal adhesions showed an increase in total area correlated with the increase in traction stress in square cells of increasing area (Fig. 4). In addition, as for traction forces, the total area of focal adhesions also increased with the distance from the corners to the center.

To test the hypothesis that the size of focal adhesions dominates over cell shape, we designed a set of substrates that maintain a constant spreading area and aspect ratio while constraining focal adhesions to different sizes. We allowed cells to spread over a constant total area of 50 μm × 50 μm on patterns consisting of a solid square, a matrix of 14 μm × 14 μm islands, or a matrix of 2 μm × 2 μm islands. Focal adhesions show a similar size on solid squares or 14 μm × 14 μm matrices. However, they are constrained to a small size on 2 μm × 2 μm squares. Average corner traction stress similarly showed no difference between cells on solid squares or on a matrix of 14 μm × 14 μm squares, but became significantly lower on 2 μm × 2 μm squares (Fig. 5).

While the above data strongly suggest that geometry sensing is mediated by focal adhesion size, traction forces could be affected by other parameters such as the continuity of adhesiveness along the cell edge. We therefore plated cells on a composite pattern where half of the 50 μm × 50 μm spreading area was solid whereas the other half consisted of a thin frame with a width of <2 μm (Supp. Fig. 2), which limited focal adhesion size in half of the cell (Supp. Fig. 2). Traction stress was similarly reduced, consistent with the hypothesis that focal adhesion size mediates geometric control of traction forces. Interestingly, we found that average corner traction stress decreases globally when compared to that on a solid 50 μm × 50 μm square, such that there is no apparent asymmetry between the frame side and the solid side in either traction forces or focal adhesion size.

Similar constraint of focal adhesion size may explain the observation that, while traction forces increase with aspect ratio over a wide range, this relationship reversed as aspect ratio became exceedingly large and the adhesion area becomes a thin line (Fig. 6). As for cells plated on a thin frame, the formation of focal adhesions and the development of traction forces are hindered by the geometry when the width of the cell approaches 10 μm (Fig. 6), which mimics cells migrating in one-dimension.

4. Discussion

Traction forces, generated by the actin-myosin II cytoskeleton [10], are transmitted to the extracellular matrix through the associated focal adhesion complexes [30]. Active traction forces are

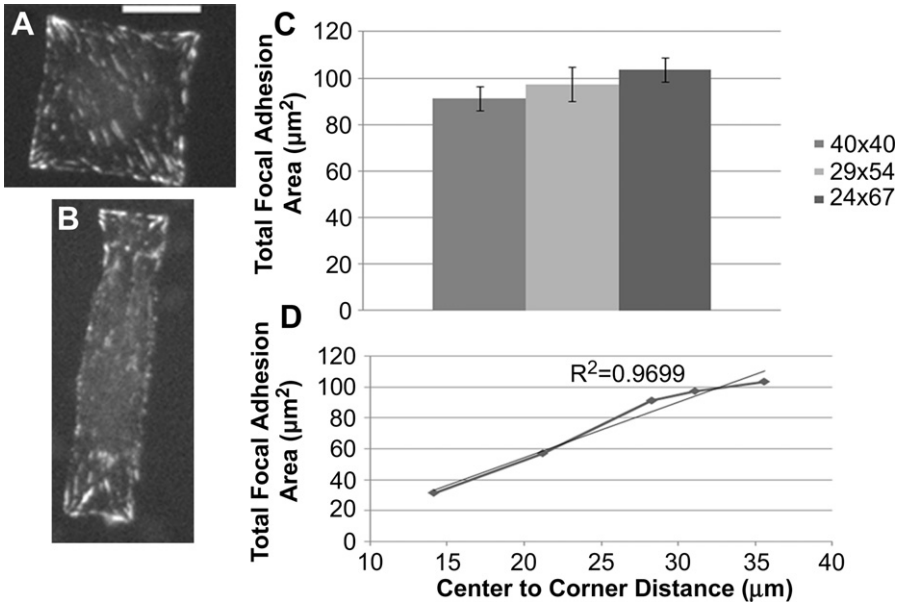

Fig. 4. Dependence of focal adhesions on cell shape. Areas of focal adhesions were measured using immunofluorescence images of paxillin (A, B), as shown for cells with an aspect ratio of 1 (A; 40 × 40 μm) or 2.8 (B; 24 × 67 μm). For rectangular cells of the same area, focal adhesions also increased with the aspect ratio (C). Across all rectangular shaped cells, the total focal adhesion area as quantified using a custom gradient based image segmentation algorithm showed a linear increase in focal adhesions with the center to periphery distance (D). Errors bars represent SEM. Scale bar, 20 μm. N = 11, 15, 20, 14, 26 for 20 × 20, 30 × 30, 40 × 40, 30 × 55, and 24 × 67 μm, respectively.

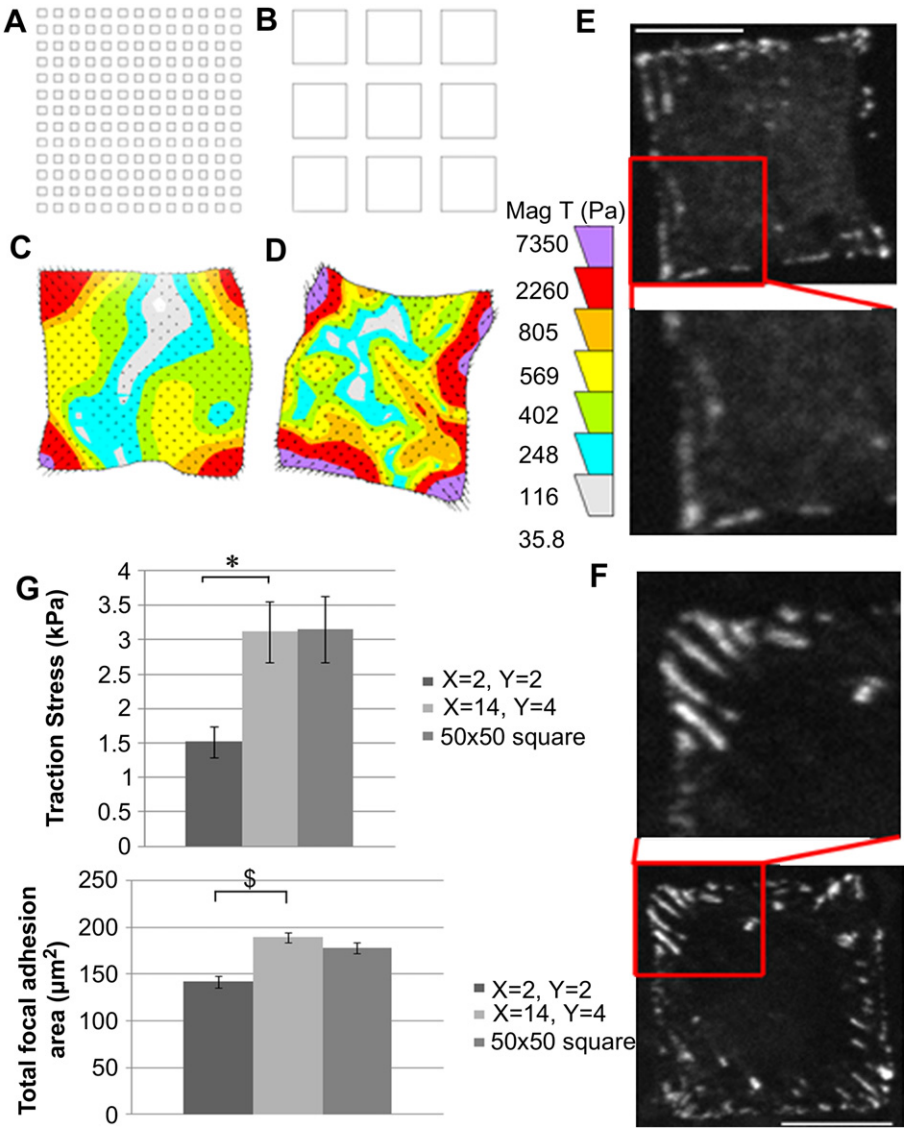

Fig. 5. Decrease of traction stress upon constraint of the focal adhesion area. Each cell occupied a 50 × 50 μm square area. Each pattern consisted of a matrix of small squares, with a side dimension *X* and a spacing *Y* covering a total area of 50 × 50 μm (A, B). For pattern 1, $X = 2$ μm, $Y = 2$ μm (A, C). For pattern 2, $X = 14$ μm, $Y = 4$ μm (B, D). Traction stress maps showed that, despite the identical spreading area and aspect ratio, traction force decreased significantly as the area of adhesive squares becomes a limiting factor for the formation of focal adhesions (note the decrease of purple in C relative to D). Immunofluorescence staining of paxillin showed a similar decrease in focal adhesions on pattern 1 relative to pattern 2 (E, F). Focal adhesions on pattern 1 appeared as isolated dots, whereas those in pattern 2 are elongated along lines of tension. Average corner traction stress indicated a decrease as adhesive areas became constrained (G). Error bars represent SEM. $N = 15, 18, 18$, for traction stress on pattern 1, pattern 2, and 50 × 50 μm square, respectively and $N = 18, 31, 17$ for focal adhesion analysis. *P*-value was calculated with Student's *T*-Test (* = $p < 0.005$, $ = $p < 0.000001$). Scale bar, 25 μm.

concentrated at the frontal periphery and are oriented toward the cell center [20,21]. Their characteristics are consistent with a propulsive role during cell migration, which has been the focus of previous analyses [21–23]. However, the present observation, that traction forces are sensitive to specific aspects of cell geometry, suggest an equally important function in detecting and controlling cell shape.

Our systematic investigations indicate that traction forces show strong dependence on the distance from the cell center to the periphery. The dependence on the total spreading area or aspect ratio, as reported previously [17,19,27–29], turns out to be secondary to center-periphery distance. Although other geometric parameters such as the overall shape of the cell may play an additional role (e.g. round versus rectangular shape, unpublished observations), this dependence of traction stress on center-periphery distance represents an economic strategy for cells to conserve energy during spreading. Inward traction forces may be analogous to surface tension for maintaining the integrity of a viscoelastic cell body [31], such that increasing forces are required as cells spread progressively from a sphere into a disk. In addition, inward traction forces elicit outward counter-forces, which in essence function like tension on a stretched tent to keep adherent cells in a spread shape. Supporting this role to maintain shape integrity, cells treated with blebbistatin, a myosin II inhibitor, took highly irregular shapes and often become fragmented [31–33].

The dependence of counter-forces, exerted by the substrate on adherent cells, on center-periphery distance may also allow a cell to detect its size and shape. Supporting this idea, responses of adherent cells to external pulling or fluid shear forces share similarities to those elicited by cell geometry, including reinforcement of the actin cytoskeleton and focal adhesions at the site of force application [11,22], and activation of similar signaling pathways [13,14]. The present results further suggest that the size of focal adhesion functions as the structural basis for geometry sensing. By

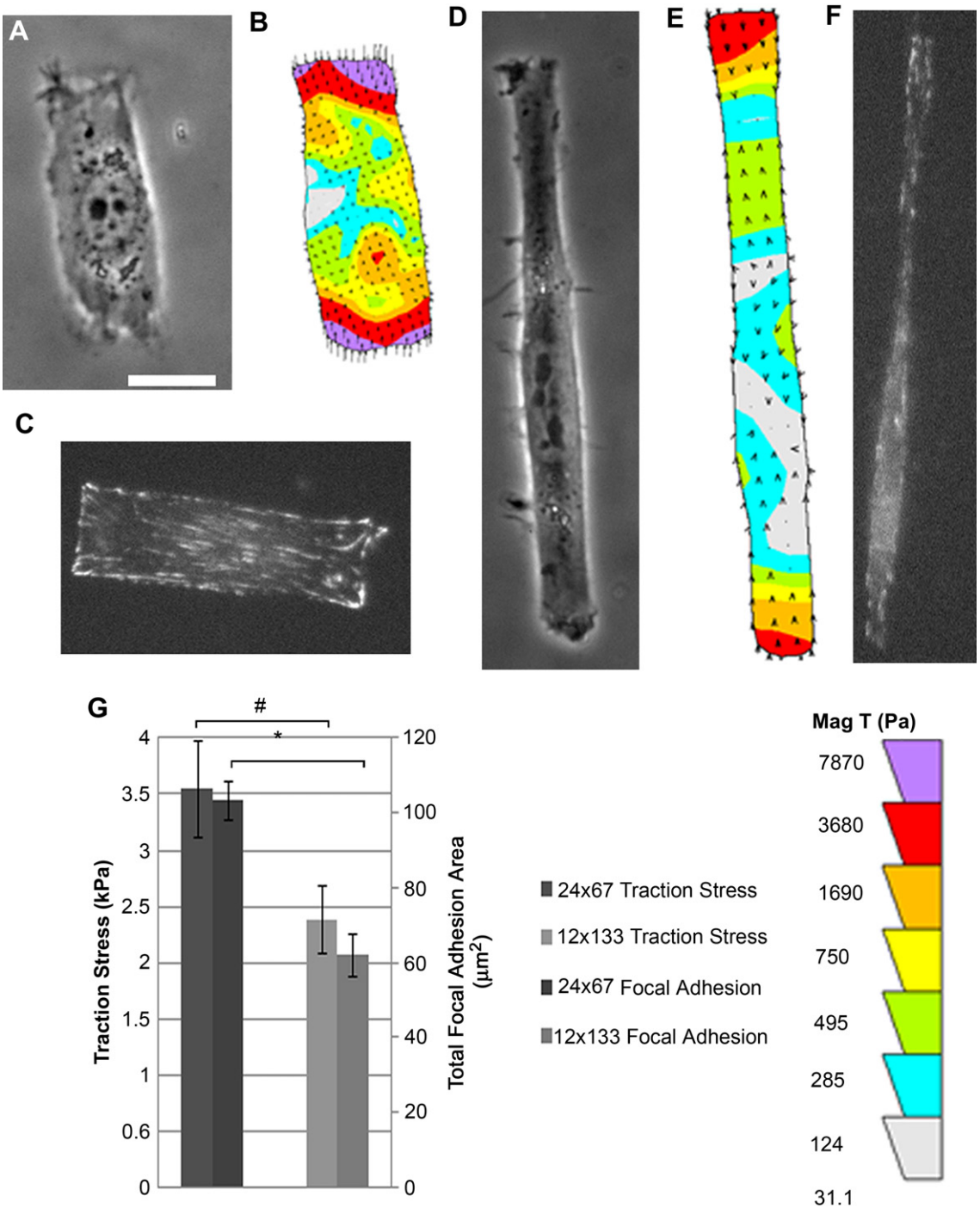

Fig. 6. Decrease in traction stress and focal adhesions for highly elongated cells. Cells were allowed to spread to the same area of 1600 μm^2 but at different aspect ratios of 2.8 (A–C), and 11 (D–F). Phase contrast images (A, C) and corresponding traction stress maps (B, E) showed a decrease in traction forces as the aspect ratio increased from 2.8 to 11 (B and E; note purple at the corners of B and lack of purple in E). Focal adhesions showed a similar decrease (B, F). The decreases of both traction stress and total focal adhesion area are statistically significant (G). *P*-value was determined using a Student's *T*-Test (* = $p < 0.005$, # = $p < 0.05$). Error bars represent SEM. $N = 19, 18$ for 24×67, and 12×133 μm, respectively for traction force and $N = 15, 26$ for focal adhesions. Scale bar, 25 μm.

manipulating focal adhesions with adhesive islands of different sizes (Fig. 5 and Supp. Fig. 2), we demonstrate that the size of focal adhesions can override the effect of overall cell geometry and thereby function as a determinant of traction stress and downstream events.

Note that the present result differs from that of Balaban et al. [34], where net traction force is proportional to the size of focal adhesion for cells spread without constraint to a steady state. This linear relationship between net forces and focal adhesion size indicates a constant traction stress (force per area) possibly due to simple mass action effect (increase of actin filaments in proportion to the size of focal adhesions). The present results instead show an increase in forces per unit focal adhesion area as the cell periphery extends, which may indicate an increase in actin filament density and/or stronger contractile forces exerted/transmitted per filament. Possibly, the size of focal adhesions and the contractility of associated cytoskeleton grow simultaneously during the assembly of nascent focal adhesions. The present results also differ

from those of Chen et al. [1], where cells were similarly plated on matrices of islands but the overall cell area appeared to play a dominant role in regulating cell growth and apoptosis. However the islands in the study were substantially larger (7 μm^2 versus 4 μm^2 for the smallest islands) than in the present study and may not have sufficiently limited the size of focal adhesions.

We propose the following mechanistic hypothesis to explain the relationship between cell shape, focal adhesions, and traction forces: 1) initially, the cell forms small focal adhesions as it adheres to the substrate, 2) these small focal adhesions produce weak traction stresses, which allow the cell to start probing mechanical properties of the substrate, 3) positive feedback from the initial probing forces serves to stimulate the assembly of the actin cytoskeleton, which in turn stimulates further spreading, formation of larger focal adhesions, and generation of stronger forces, and 4) this positive cycle continues, leading to a continuous increase in the size of focal adhesions and magnitude of traction stress until the cell reaches its limit of spreading or fills up the adhesive area.

Interestingly geometry sensing involves both global and local components. In addition to local geometry-dependent concentration of traction forces and focal adhesions at corners of rectangles, there is a global coordination as evidenced by the decrease in focal adhesions and traction forces throughout the cell when the adhesion of half of a cell is confined to a thin frame. Local responses may involve the activation of enzyme or substrate activities as a result of force-induced protein conformational change [35–37], and may include the Rho family GTPases [38], or components of tyrosine kinase pathways such as P130Cas [37]. Downstream signals may then propagate globally, reaching the nucleus via the Erk1/2 pathway to regulate gene expression [39]. In addition, due to the viscoelastic nature of the cytoplasm, mechanical forces propagate throughout the cell causing global cross-talks among different regions [40]. The law of physics mandates that these forces be balanced against each other globally to maintain overall mechanical neutrality.

A similar mechanism may serve as a means for adhesive cells to detect and respond to substrate rigidity. Stiff substrates induce strong positive feedback and promote cell spreading, large focal adhesions, large stress fibers, and strong traction forces [41–43]. Conversely, weak mechanical signals on soft substrates would limit the overall feedback, the size of focal adhesions and stress fibers, and the magnitude of traction forces, thereby the spread area. This general mechanism, in which cells respond to substrate stiffness and cell shape with a common signaling pathway, is also consistent with the observation that well spread cells on soft matrices behave similarly to moderately spread cells on stiffer matrices, as reported with both fibroblasts and mesenchymal stem cells [1,6,43,44].

The present results have important practical implications. The pivoting role of focal adhesion size explains the differences between cells on 2-D surfaces and those adhering to a matrix of fibers [45], where focal adhesions are confined to a small size along the thin fiber. It also explains why cells on thin lines or with a very large aspect ratio (Fig. 6) behave strikingly similar to those in 3-D extracellular matrix [46]. In addition, our results indicate that cell behavior may be controlled by a combination of shape, size, adhesion pattern, rigidity, contractility, external forces, and chemical factors. As these parameters share a common basic mechanism of mechanosensing, they may compensate one another such that similar differentiation fates may be reached under a range of conditions. This general principle should guide regenerative medicine to tailor the treatment for specific needs. The output and input of mechanical forces, whether they are controlled by chemicals, topography, rigidity, or external forces, serve as the key parameter for obtaining the desired outcome of cell growth, differentiation, and migration.

5. Conclusion

A systematic study of the effect of adherent cell shape on traction stresses using a new hydrogel micropatterning method led to the conclusion that traction stress correlates linearly with the center-to-corner distance of rectangular cells. Shape control of traction stress is in turn mediated by the regulation of focal adhesion size, which dominates over the overall cell size and shape. Importantly, this same mechanism is capable of detecting a wide range of mechanical and geometrical signals.

Acknowledgements

We thank Prof. Micah Dembo, Boston University, for providing the LIBTRC program package for computing traction forces. This work was supported by grant GM-32476 from the National Institutes of Health to Y.L.W.

Appendix

Figures with essential color discrimination. Fig. 2 in this article are difficult to interpret in black and white. The full color images can be found in the online version, at doi:10.1016/j.biomaterials.2010.11.044.

Appendix. Supplementary data

Supplementary data related to this article can be found online at doi:10.1016/j.biomaterials.2010.11.044.

References

[1] Chen CS, Mrksich M, Huang S, Whitesides GM, Ingber DE. Geometric control of cell life and death. Science 1997;276(5317):1425–8.
[2] Singhvi R, Kumar A, Lopez GP, Stephanopoulus G, Wang DI, Whitesides GM, et al. Engineering cell shape and function. Science 1994;264(5159):696–8.
[3] Baill M, Yan L, Whitesides GM, Condeelis GS, Segall JE. Regulation of protrusion shape and adhesion to the substratum during chemotactic responses of mammalian carcinoma cells. Exp Cell Res 1998;241(2):285–99.
[4] Dike L, Chen CS, Mrksich M, Tien J, Whitesides GM, Ingber DE. Geometric control of switching between growth, apoptosis, and differentiation during angiogenesis using micropatterned substrates. In Vitro Cell Dev Biol 1999;35(8):441–8.
[5] Chen CS, Mrksich M, Huang S, Whitesides GM, Ingber DE. Micropatterned surfaces for control of cell shape, position, and function. Biotechnol Prog 1998;14(3):356–63.
[6] McBeath R, Pirone DM, Nelson CM, Bhadriraju K, Chen CS. Cell shape, cytoskeletal tension, and RhoA regulate stem cell lineage commitment. Dev Cell 2004;6(4):483–95.
[7] Kilian KA, Bugarija B, Lahn BT, Mrksich M. Geometric cues for directing the differentiation of mesenchymal stem cells. Proc Natl Acad Sci U S A 2010;107(11):4872–7.
[8] Beningo KA, Hamao K, Dembo M, Wang Y-L, Hosoya H. Traction forces of fibroblasts are regulated by the Rho-dependent kinase but not by the myosin light chain kinase. Arch Biochem Biophys 2006;456(2):224–31.
[9] Harris AK, Wild P, Stopak D. Silicone rubber substrata: a new wrinkle in the study of cell locomotion. Science 1980;208(4440):177–9.
[10] Kolega J, Janson LW, Taylor DL. The role of solation-contraction coupling in regulating stress fiber dynamics in nonmuscle cells. J Cell Biol 1991;114(5):357–63.
[11] Riveline D, Zamir E, Balaban NQ, Schwarz US, Ishizaki T, Narumiya S, et al. Focal contacts as mechanosensors: externally applied local mechanical force induces growth of focal contacts by an mDia1-dependent and ROCK-independent mechanism. J Cell Biol 2001;153(6):1175–86.
[12] Wang N, Ingber DE. Control of cytoskeletal mechanics by extracellular matrix, cell shape, and mechanical tension. Biophys J 1994;66(6):2181–9.
[13] Davies PF. Overview: temporal and spatial relationships in shear stress-mediated endothelial signalling. J Vasc Res 1997;34(3):208–11.
[14] Azuma N, Akasaka N, Hiroyuki K, Ikeda M, Gahtan V, Sasajima T, et al. Role of p38 MAP kinase in endothelial cell alignment induced by fluid shear stress. Am J Physiol Heart Circ Physiol 2001;280(1):H189–97.
[15] Reinhart-King CA, Dembo M, Hammer DA. Endothelial cell traction forces on RGD-derivatized polyacrylamide substrata. Langmuir 2003;19(5):1573–9.
[16] Li F, Li B, Wang QM, Wang JHC. Cell shape regulates collagen type I in human tendon fibroblasts. Cell Motil Cytoskeleton 2008;65(4):332–41.

[17] Wang N, Ostuni E, Whitesides GW, Ingber DE. Micropatterning tractional forces in living cells. Cell Motil Cytoskeleton 2002;52(2):97–106.
[18] Reinhart-King CA, Dembo M, Hammer DA. The dynamics and mechanics of endothelial cell spreading. Biophys J 2005;89(1):676–89.
[19] Tan JL, Tien J, Pirone DM, Gray DS, Bhadriraju K, Chen CS. Cells lying on a bed of microneedles: an approach to isolate mechanical force. Proc Natl Acad Sci U S A 2003;100(4):1484–9.
[20] Lee J, Leonard M, Oliver T, Ishihara A, Jacobson K. Traction forces generated by locomoting keratocytes. J Cell Biol 1994;127(6 Pt 2):1957–64.
[21] Dembo M, Wang Y-L. Stresses at the cell-to-substrate interface during locomotion of fibroblasts. Biophys J 1999;76:2307–3216.
[22] Beningo KA, Dembo M, Kaverina I, Small JV, Wang Y-L. Nascent focal adhesions are responsible for the generation of strong propulsive forces in migrating fibroblasts. J Cell Biol 2001;153(4):881–8.
[23] Munevar S, Wang Y-L, Dembo M. Distinct roles of frontal and rear cell-substrate adhesions in fibroblast migration. Mol Biol Cell 2001;12(12):3947–54.
[24] Damljanović V, Lagerholm DC, Jacobson K. Bulk and micropatterned conjugation of extracellular matrix proteins to characterized polyacrylamide substrates for cell mechanotransduction assays. Biotechniques 2005;39(6): 847–51.
[25] Wang Y-L, Pelham RJ. Preparation of a flexible, porous polyacrylamide substrate for mechanical studies of cultured cells. Meth Enzymol 1998;298: 489–96.
[26] Frey MT, Engler AJ, Discher DE, Lee J, Wang Y- L. Microscopic methods for measuring the elasticity of gel substrates for cell culture: microspheres, microindenters, and atomic force microscopy. Methods Cell Biol 2007;83: 47–66.
[27] Parker KK, Brock AL, Brangwynee C, Mannix RJ, Wang N, Ostuni E, et al. Directional control of lamellipodia extension by constraining cell shape and orienting cell tractional forces. FASEB J 2002;16(10):1195–205.
[28] Thery M, Pepin A, Dressaire E, Chen Y, Bornens M. Cell distribution of stress fibres in response to the geometry of the adhesive environment. Cell Motil Cytoskeleton 2006;64(6):341–55.
[29] Novak IL, Slepchenko BM, Mogilner A, Loew LM. Cooperativity between cell contractility and adhesion. Phys Rev Lett 2004;93(26 Pt 1):268109.
[30] Geiger B, Bershadsky A. Assembly and mechanosensory function of focal contacts. Curr Opin Cell Biol 2001;13(5):584–92.
[31] Mader CC, Hinchcliffe EH, Wang Y-L. Probing cell shape regulation with patterned substratum: requirement of myosin II-mediated contractility. Soft Matter 2007;3(3):357–63.
[32] Huxley HE. The mechanism of muscular contraction. Science 1969;164 (3886):1356–66.
[33] Totsukawa G, Wu Y, Sasaki Y, Hartshorne DJ, Yamakita Y, Yamashiro S, et al. Distinct roles of MLCK and ROCK in the regulation of membrane protrusion and focal adhesion dynamics during cell migration of fibroblasts. J Cell Biol 2004;164(3):427–39.
[34] Balaban NQ, Schwarz US, Riveline D, Goichberg P, Tzur G, Sabany I, et al. Force and focal adhesion assembly: a close relationship studied using elastic micropatterned substrates. Nat Cell Biol 2001;3(5):466–72.
[35] Sai X, Naruse K, Sokabe M. Activation of pp60src is critical for stretch-induced orienting response in fibroblasts. J Cell Sci 1999;112(Pt 9):1365–73.
[36] Johnson RP, Craig SW. F-actin binding site masked by the intramolecular association of vinculin head and tail domains. Nature 1995;373(6511):261–4.
[37] Sawada Y, Tamada M, Dubin-Thaler BJ, Cherniavskaya O, Sakai R, Tanaka S, et al. Force sensing by mechanical extension of the Src family kinase Substrate p130Cas. Cell 2006;127(5):1015–26.
[38] Chrzanowska-Wodnicka M, Burridge K. Rho-stimulated contractility drives the formation of stress fibers and focal adhesions. J Cell Biol 1996;133(6): 1403–15.
[39] Numaguchi K, Eguchi S, Yamakawa T, Motley ED, Inagami T. Mechanotransduction of rat aortic vascular smooth muscle cells requires RhoA and intact actin filaments. Circ Res 1999;85(1):5–11.
[40] Wang N, Suo Z. Long-distance propagation of forces in a cell. Biochem Biophys Res Commun 2005;328(4):1133–8.
[41] Pelham RJ, Wang YL. Cell locomotion and focal adhesions are regulated by substrate flexibility. Proc Natl Acad Sci U S A 1997;94(25):13661–5.
[42] Wang HB, Dembo M, Wang YL. Substrate flexibility regulates growth and apoptosis of normal but not transformed cells. Am J Physiol 2000;279 (5):C1345–50.
[43] Yeung T, Georges PC, Flanagan LA, Marg B, Ortiz M, Funaki M, et al. Effects of substrate stiffness on cell morphology, cytoskeletal structure, and adhesion. Cell Motil Cytoskeleton 2005;60(1):24–34.
[44] Engler AJ, Sen S, Sweeney HL, Discher DE. Matrix elasticity directs stem cell lineage specification. Cell 2006;126(4):677–89.
[45] Fraley SI, Feng Y, Krisnamurthy R, Kim D-H, Celedon A, Longmore GD, et al. A distinctive role for focal adhesion proteins in three-dimensional cell migration. Nat Cell Biol 2010;12(6):598–605.
[46] Doyle AD, Wang FQ, Matsumoto K, Yamada KM. One-dimensional topography underlies three-dimensional fibrillar cell migration. J Cell Biol 2009;184 (4):481–90.